Nanostructuring with Nanojoule Femtosecond Laser Pulses

R. LE HARZIC[*, **], M. STARK[*], H. SCHUCK[*], P. BECKER[*],
E. LAI[*], D. BRUNEEL[***], F. BAUERFELD[*], D. SAUER[*], T. VELTEN[*] and K. KÖNIG[*]

[*] *Fraunhofer Institute of Biomedical Technology (IBMT), Ensheimer strasse 48*
D-66386 St. Ingbert, Germany
E:mail: ronan.leharzic@ibmt.fraunhofer.de
[**] *JenLab GmbH, Schillerstrasse 1, D-07745 Jena, Germany, www.jenlab.de*
[***] *Laboratoire Hubert Curien - UMR 5516, 18 rue Benoît Lauras ,*
42000 Saint Etienne, France

Sub-wavelength multiphoton nanoprocessing of silicon wafers, direct nanowriting of metals, borosilicate glass or polymers, laser processing for nanofluidics applications as well as 3D maskless lithography by two-photon polymerization have been performed using several compact near infrared MHz femtosecond lasers as tuneable turn-key, one-box Chameleon (coherent) and Mai-Tai (spectra physics) oscillators as well as a special femtoTrain system (High Q laser production GmbH). The lasers were coupled with the scanning microscopes *FemtOcut* (JenLab GmbH) and a modified ZEISS LSM510-NLO system. MHz femtosecond laser pulses with nanojoule photon energies can be considered as novel tools for nanoprocessing in material science, nanobiotechnology and nanomedicine.

DOI: 10.2961/jlmn.2008.02.0009

Keywords: MHz femtosecond lasers, multiphoton microscopes, nanoprocessing, nanopatterning, two-photon polymerization, rapid prototyping

1. Introduction

Femtosecond laser micromachining has become increasingly important in recent years for many fields [1-7]. Laser ablation, because of its non-contact nature, allows the micromachining and surface patterning of materials with minimal mechanical and thermal deformation. It is now well known that for many of these applications, the femtosecond regime offers advantages over the nanosecond regime. These advantages lie in its ability to deposit energy into a material in a very short time period, before thermal diffusion can occur. As a result, the heat-affected zone, where melting and solidification can occur, is significantly reduced. Smaller feature sizes, greater spatial resolution, and better aspect ratios can hence be achieved. The energy density best conditions for micromachining are achieved near the ablation threshold [8-10]. Compact femtosecond laser resonators working in NIR at high repetition rates have successfully been applied to perform two-photon fluorescence and second harmonic generation (SHG) microscopy and tissue imaging [11-13]. Pulses from these non amplified laser resonators can also be used to perform multiphoton ablation. Pulse energies in the sub-3 nJ range are sufficient to induce multiphoton ionization when using high NA objectives in order to obtain transient TW/cm^2 laser intensities. This was shown in biological material including DNA molecules and biological tissues [14-17]. By exploiting this multiphoton effect we were able to perform patterning of several types of material with submicron resolution. Nanostructuring of a variety of materials is gaining widespread importance owing to ever-increasing potential applications of nanostructures in numerous fields as nanolithography, controlled nanodeposition, high-density data storage, nanooptoelectronics, counterfeiting, micro-nanofluidics as well as various biotechnology related applications [18].

Here we report on the use of titanium: sapphire and Yb laser resonators in combination with compact microscope systems for nanoprocessing.

An exhaustive overview of our results and different applications in the miniaturized world is given in this paper.

2. Material and methods

2.1 Lasers

To generate the required intensity for two-photon excitation to take place, 2 turn-key mode-locked femtosecond laser sources with ultrashort pulses were used (Mai Tai, Spectra- Physics, USA and Chameleon, Coherent Inc,

USA). Both are tuneable Ti-sapphire lasers providing an average power of 1.5W at 800nm at a repetition rate of 80MHz and with a pulse duration of 100fs for the Mai Tai one and with 170 fs pulse duration, a repetition rate of 90 MHz and a maximum mean power of 1750 mW at 800 nm for the Chameleon one.
Ytterbium-doped gain media lasers are a powerful technology while efficient pumping is done at 910 nm or near of 975nm wavelengths which correspond to classical telecom wavelengths. So it becomes easy to use diodes to pump directly the ytterbium-doped crystal which simplify and make reliable systems. The diode-pumped solid state laser based on Ytterbium and SESAM technology used for our application is a femtoTRAIN IC221 oscillator (High Q Laser Production GmbH, Austria) which as particularity can deliver 3 wavelengths, 1035 nm (fundamental), 517 nm (SHG) and 345 nm (THG) at a repetition rate of 20 MHz and with typical pulse duration of 230 fs.

2.2 Microscopy systems

The Yb oscillator was introduced into the optical system *FemtOcut* (JenLab GmbH) based on a standard fluorescence microscope with a galvo-scanning module attached to the side port (setup 1). The beam scanning module consists of beam deflection mirrors, scan optics including an 1:6 beam expander, a motorized beam attenuator, a beam shutter and a fast x,y galvo scanner (GSI Lumonics, USA). For nanostructuring with different wavelengths, the laser beam was directly coupled in the microscope by the rear side without the beam scanning module to overcome problems of complicate optical paths and losses. The samples were mounted on a three-motorized-axes system x,y,z computer controlled with 0.3 µm accuracy (Feinmess Dresden GmbH, Germany). Specific optics for IR, green and UV as mirrors, beam splitter and filters have been used. An IR and UV coated Glan Calcite polarizers were introduced in the laser path to allow the control of the laser power. Focusing oil objective with a numerical aperture of 1.3 (Zeiss, Germany) and water objective 0.9 (Zeiss, Germany) have been used.
The Mai Tai and Chameleon laser systems were coupled into 2 microscopes systems: first, an inverted laser scanning microscope for experiments (Zeiss LSM 510 NLO META). A fully adjustable attenuator was also used to control the mean laser power experiments. In order to reach the ablation threshold of materials, focusing oil objective with high numerical aperture of 1.3 oil as describe above was used under oil environment. The laser beam was expanded by an 1:4 telescope. The Scanning microscope was alternately coupled with the Chameleon laser (setup 2) and the Mai-Tai laser (setup 3)
The fourth configuration employed in this study is a modified inverted microscope (Axiovert 200, Zeiss AG, Germany) outfitted with a fluorescence imaging module (TauMap, JenLab GmbH, Germany) which was only coupled with the Mai Tai laser (setup 4). In contrast with the LSM-510 META, the laser beam is held fixed vertically while the specimen is shifted in the horizontal plane using a piezoelectric nanopositioning stage (Feinmess Dresden GmbH, Germany). An external z-stage (Physik Instrumente GmbH, Germany) controls the vertical movement of the objective lens. Fig. 1 shows the common principle of the different lasers coupled with microscopes described above for micro-nanostructuring.

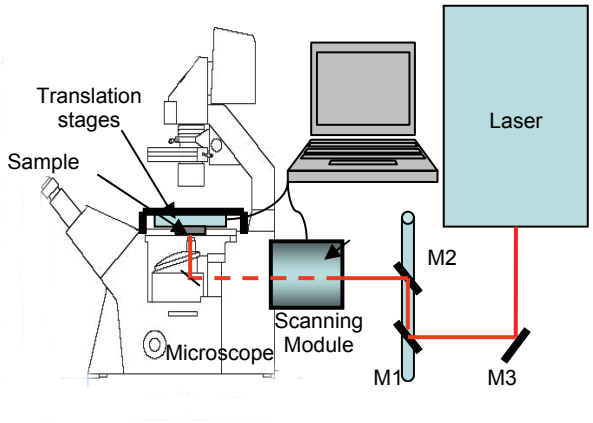

Fig 1 Experimental setup for nanostructuring applications.

3. Results and discussions

3.1 Direct nanostructuring of materials

A principal challenge facing nanotechnology is consistently producing well-defined features much smaller than the wavelength of visible light and to reach dimensions smaller than the diffraction limit. One approach to achieve this is to use optical breakdown, a process through which localized plasma is generated when matter is subjected to focused high-power laser pulses and this is particularly effective using very short pulses which allow the process to be limited to regions smaller than the spot size of the focused laser near the ablation thresholds of materials (i.e. to obtain the smallest width of the Gaussian intensity distribution beyond the ablation threshold) The main results have been obtained using the setup 1.

3.1.1 Borosilicate glass structured at the surface

In the fig 2, a spiral pattern has been achieved in the infrared at 1035 nm with an energy per pulse of 6 nJ. The width of the structured channel is in the range of 800 nm smaller than the wavelength.

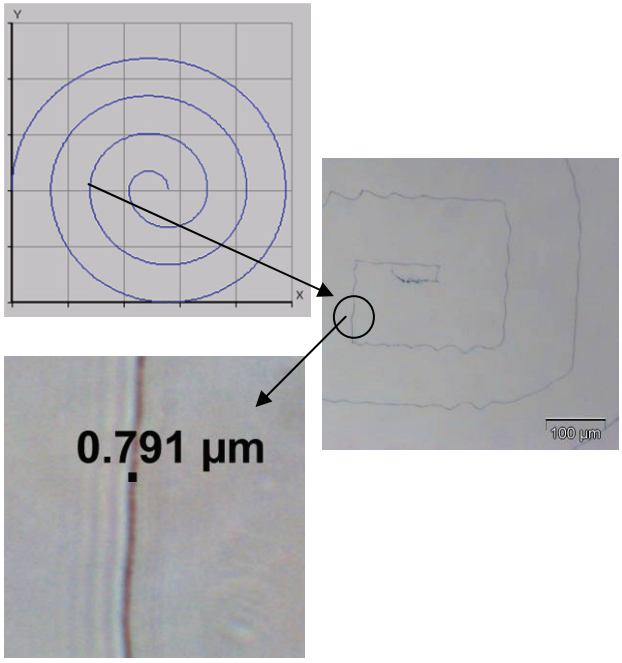

Fig. 2 Spiral pattern in borosilicate glass with sub-µm typical line width performed at 1035 nm.

In the fig 3, a groove has been achieved at half the fundamental wavelength at 517 nm with an energy per pulse of 3.5 nJ. The width of the structured channel is in the range of 600 nm.

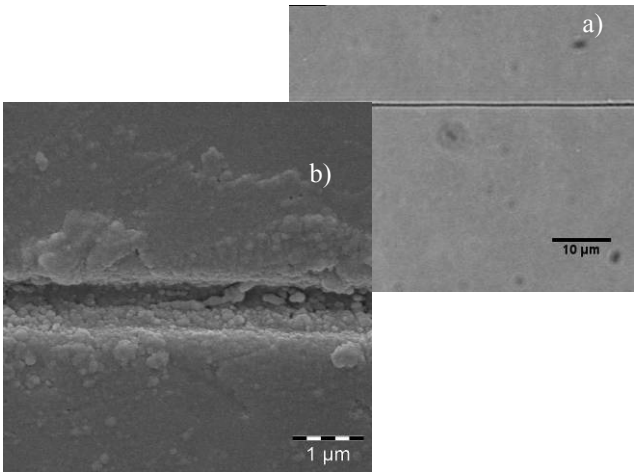

Fig 3 0.6 µm channel width was achieved at 517 nm. (a) optical image, (b) SEM image.

3.1.2 Nanostructuring in the bulk of borosilicate glass and polymer

Some test have been performed in the bulk of a borosilicate glass to perform small feature as diffraction grating as depicted in the fig. 4 with an energy per pulse of 2 nJ at a wavelength of 1035 nm. The width of the line is almost half less than the wavelength.

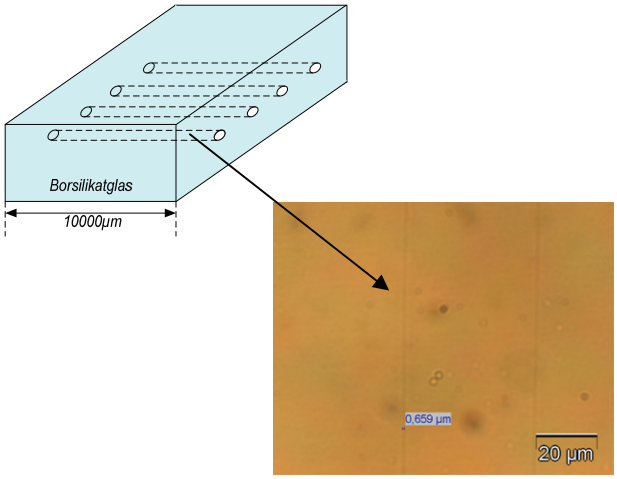

Fig 4 Intrabulk 0.6 µm channel width processed per at 1035 nm in the bulk of borosilicate glass.

Nano-gratings have been written within the bulk of the polymer foil (thickness of 50 to 100 µm, first layer of a credit card (fig.5 (a)) using low pulse energies in the range of 2 nJ and single line scanning [19] at 1035 nm. An image of the sub-µm lines written in the bulk is given in (b). By illuminating with a He-Ne laser or a simple laser diode pen, one can obtain diffraction patterns (c). These nano-gratings are quasi undetectable with eyes and are of prime interest for bank security and cards counterfeiting.

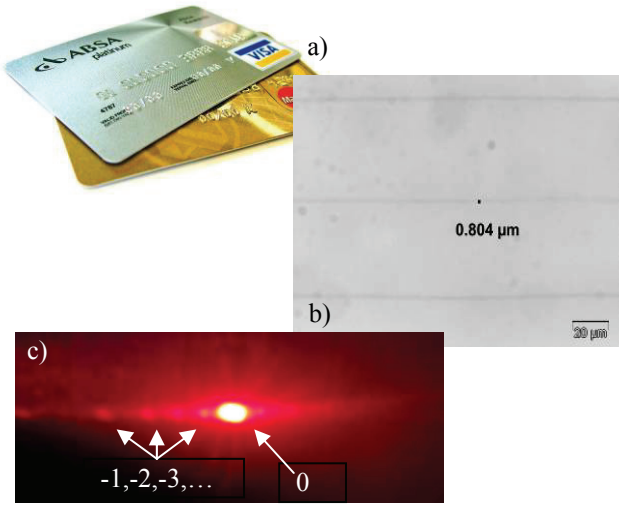

Fig 5 Nanostructuring of diffraction gratings in the bulk of polymer foil (thickness of 50 to 100 µm), first layer of a credit card (a) using IR low pulse energies in the range of 2 nJ and single line scanning. (b) Optical image of the 800 nm wide grooves, (c) diffraction pattern.

3.1.3 Nanostructuring of metal: gold thin film

Fig. 6 and 7 show efficient nanostructuring of channels on a thin gold film of approximately 1 µm thick on a Cr substrate performed respectively at 1035 nm and 3 nJ/pulse

and at 517 nm and 2 nJ/pulse. These results demonstrate the ability of the technique to write very small features in a thin metal film with sub-µm resolution, even smaller using green light compared to infrared.

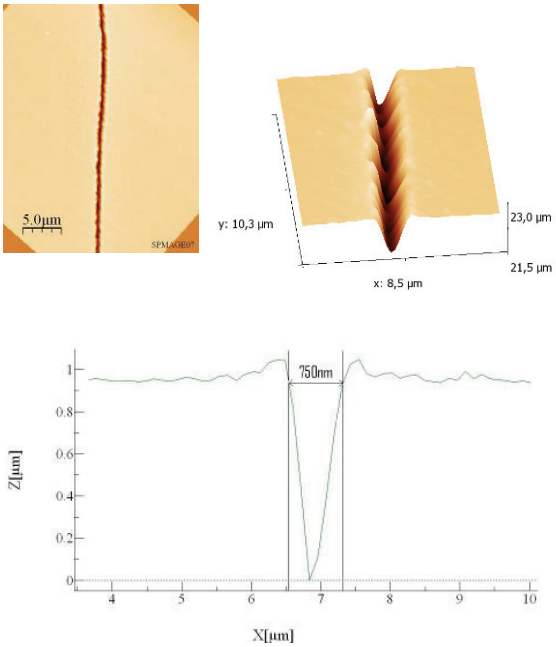

Fig 6 Nanostructuring of a groove in a gold thin film at 1035 nm and 3 nJ/pulse. Cut size is 750 nm.

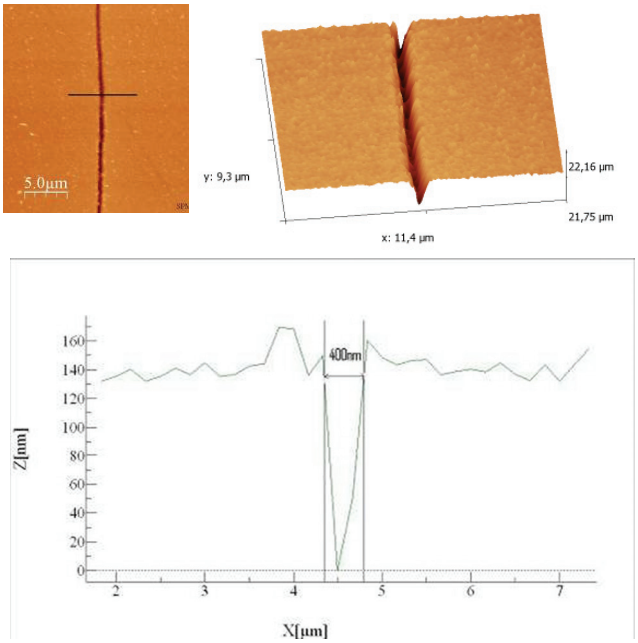

Fig 7 Nanostructuring of a groove in a gold thin film at 517 nm and 2 nJ/pulse. Cut size is 400 nm.

3.1.4 Nanostructuring of silicon

Laser-induced surface structuring in silicon has been extensively studied [20-22]. Silicon, as the most important material for the semi-conductor industry, presents some specific characteristics when irradiating with ultra-short laser pulses at low fluence. Spontaneous periodic surface structures or ripples are observed. Previous results is shown in the fig 8, have demonstrated for the first time to our knowledge the ability to perform sub-100 nm structures with the setup 2 [23]. One line scan was performed at a scan speed of approximately 1 mm/s but at very low energy/pulse of 3.5 nJ which represent a fluence close to the ablation threshold (100-300 mJ/cm^2 depending on the number of pulses). SEM images have been taken on silicon samples after etching with ammonium fluoride to remove recast, melted matter and nanoparticles at the border and in the structures. Most interestingly, the period of the surface ripples were found to be in the order of 70 to 100 nm. That's about 10 times less than the wavelength which was 800 nm. The direction of the induced periodic structures is parallel to the laser polarization.

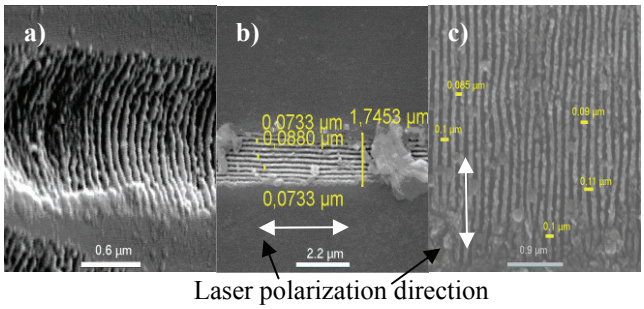

Fig 8 SEM images of the periodic structures formed in oil confinement after laser irradiation (90 MHz, 3.5 nJ/pulse, 350 fs, 170 fs, 800 nm); use of a 40x oil focusing objective (NA: 1.3) [23].

Further investigations have been performed with the experimental setup 1 at 1035 nm and 347 nm. Results obtained at 1035 nm as shown in fig. 9. Periodic structures of about 400 nm have been performed at an energy of 6 nJ/pulse (2 to 3 times less than the wavelength).

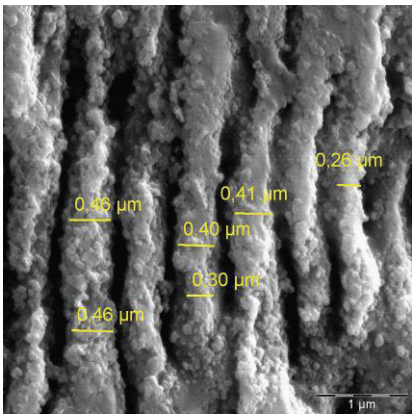

Fig 9 SEM images of the periodic structures formed after laser irradiation at 1035 nm and 6 nJ/pulse.

Results obtained with UV irradiation at 345 nm and with 1 nJ/pulse are shown in fig. 10. No periodic structures are observable but grooves of about 150 nm can be directly performed (3 times less than the wavelength). The forma-

tion of nanostructures on silicon depends strongly on the wavelength of the laser. The physical phenomenon induced in the UV seems to be different than with IR irradiation.

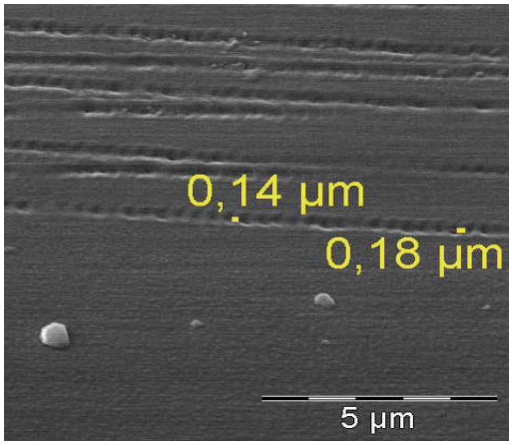

Fig 10 SEM images of the grooves formed after laser irradiation at 347 nm and 1 nJ/pulse.

3.1.5 Towards micro-nanofluidics.

Complex microfluidic devices are of broad interest for basic research and have large field of applications including diagnostics, chemical analysis, sensors drug discovery, and microreactors. Efforts to produce highly complex and high density microfluidic devices capable of generalized chemical processing are challenged by space limitations and the inability to cross two planar fluidic channels without mixing. Yet most microfabrication methods are inherently planar and few are capable of submicrometer dimensions. Femtosecond laser-assisted micromachining is a promising alternative technique to produce 3-D devices in transparent dielectrics [24-27]. The intensity required is achieved by tightly focusing the laser beam. Short pulses also minimize the heat effect and allow modification to be controlled**.** We present here some preliminary investigations to prototype three-dimensional channels with micro-diameter in glass at 515 nm and 20 MHz with 7.5 nJ/pulse [28]. The principle of the experimental setup is describe in fig. 11. Typical diameters of the channels as shown in fig. 12 are in the range of 2 to 3 µm actually. Further investigations have to be performed in this way.

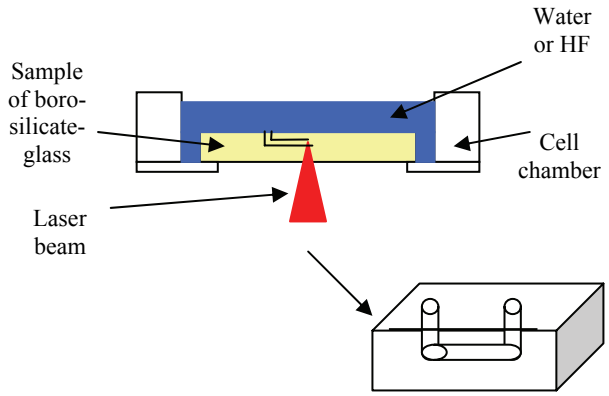

Fig 11 Principle of the experimental setup.

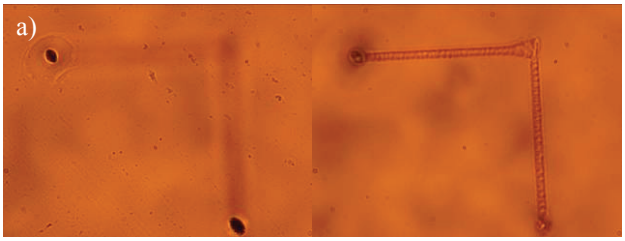

At the surface In the bulk

Fig 12 (a) Images of a 3D channel performed in the bulk of a PMMA at 515 nm and 7.5 nJ/pulse, (b) a cut has been made on the slide to observe the characteristics of the channels.

3.2 Prototyping of 3D micro-nano nanostructures

Photoresist is widely used in the microtechnology industry as a mean to transfer specific structural patterns onto the substrate. Polymerisation can be induced in the photoresist where the local intensity exceeds the minimum polymerisation threshold. By exploiting this attribute, it is possible to achieve structural resolution smaller than the diffraction limit. Some recent works describe the production of real 3D structures in photo resists by two-photon-polymerisation (2PP). Since the two photon effect occurs only in a small area of the focus, this method allows the manufacturing of very small 3D geometries down to 100 nm.

A common photoresist SU-8 is typically exposed to 365 nm light during 2D photolithography procedures. NIR femtosecond laser pulses (setup 3) were used at a typical wavelength of 730 nm to expose the photoresist by a two-photon absorption process and realized maskless 3D photolithography. A typical mean power of 20 mW (250 pJ pulse energy) was chosen. Sub-200nm stuctures can be created as depicted in fig. 13 [29].

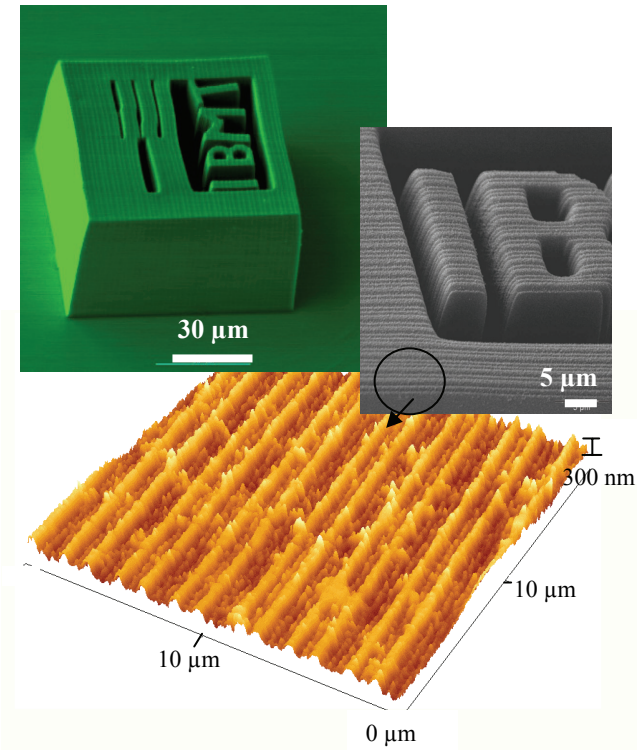

Fig 13 Two-photon photopolymerization of SU-8 photoresist. Sub-200nm periodic structures were created.

An example of a grid pattern performed in SU-8 with high aspect ratio walls is shown in fig. 14. The height of the structure is about 200 µm. The smallest wall structure is less than 400 nm in width.

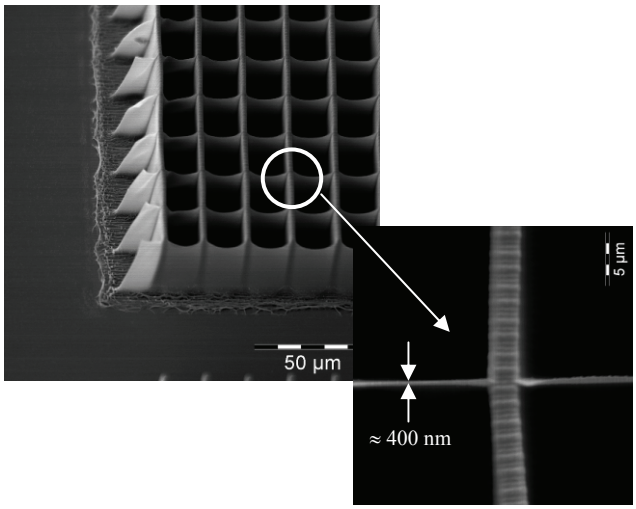

Fig 14 Grid pattern performed byTwo-photon photopolymerization of SU-8 photoresist.

The presented process is a powerful tool for rapid fabrication of 3D geometries. The manufacturing of different surfaces and volumes are possible down to sub µm range. One of the potential applications of nanotopography features is the manipulation of biological specimens as will be discussed in the following paragraph.

3.3 Influence of nanostructured surfaces on cell behavior [30]

Numerous research groups are interested on studying the interaction of cells on structured surfaces, because cues from these surfaces could have significant impact on cell adhesion, migration, and proliferation. The term "contact guidance" is frequently used to describe this type of cell behaviour. A list of diverse structured topographies from various groups is compiled by Flemming *et al* [31], and an overview of their influence on cell behaviour is provided by Curtis *et al* [32].

Typical spiral and concentric structures were performed on SU-8 photoresist substrate as shown in fig. 15 using the microscope coupled with the Mai Tai laser as depicted in setup 4. The height of the structures is typically 7µm. On one of the substrate, two concentric circles of unequal heights (5µm difference in height) are placed close to each other to produce an overlap region (see Fig. 15.b). The width of the structures measured from light microscope is about 5µm.

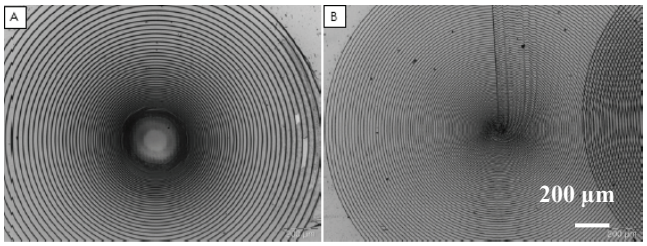

Fig 15 Typical spiral and concentric structures performed on SU-8 photoresist substrate The height of the structures is typically 7µm. The distance between two adjacent circles increase with remotness from the center.

Chinese hamster ovary cells (CHO-K1) were putted on the spiral pattern presented above and as depicted in fig. 16, the evolution of cells orientation with time was studied. The standard laboratory cell line exhibited good growth on the microstructures. As shown in fig. 16(a), cells on plain surfaces were randomly oriented while those on the microstructures tend to have an elongated body that followed the curvature of the structures. This observation was further confirmed as observed in fig. 16(b), (c) and (d) and on the SEM image (fig. 17).

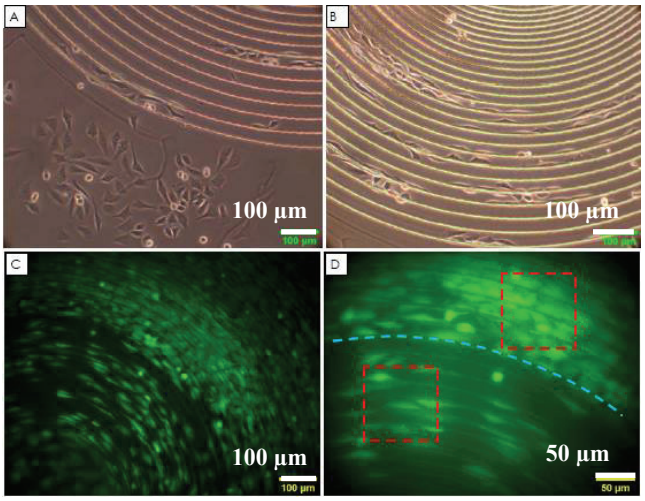

Fig. 16 (a) 48 hours post-seeding. Comparison of cells on plain surface and spirals. (b) 48 hours postseeding. Most of the cells have attached to structures with larger radius. (c) 96 hours post-seeding (stained). A difference in pop lation density is observed. (d) 96 hours post-seeding (stained). A close-up showing the change in cell density at radius 480 µm (blue line). Red squares are sample regions.

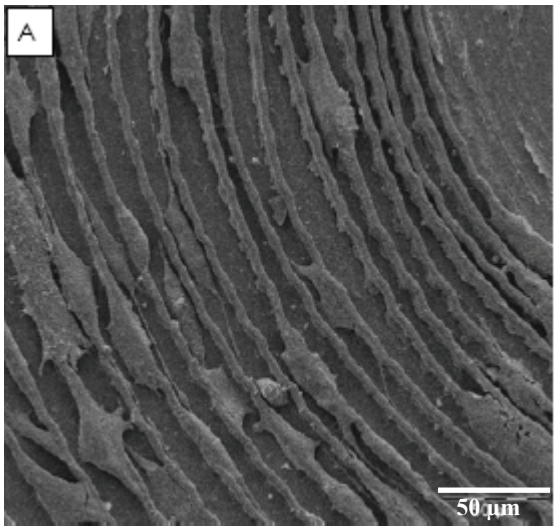

Fig 17 Scanning electron microscope images of Chinese hamster ovary cells. Cells are seen and oriented between and above the structures.

4. conclusion

Here we have demonstrated efficient nanostructuring of various materials as metals, polymer, silicon or glass by using un-amplified nJ femtosecond pulses and laser scanning microscopes. Miniaturisation is an attribute of today's photonic industry, determining an intense and global effort in micro and nano technology, and in this context, materials micro/nano structuring has become the backbone of rapidly expanding application areas in emerging technologies. Further progress in telecommunications, optics, electronics, biomaterials, medicine, and transport strongly depends on the availability of reliable and rapid processing techniques. Laser-based micro nano technology holds great promises and the evolution will be dictated by the development of inexpensive yet precise processing tools that can develop and structure materials with a high degree of controllability, accuracy, and reduced residual damage.

5. References

[1] C. Momma, B. N. Chichkov, S. Nolte, F. von Alvensleben, A. Tunnermann, H. Welling, B. Wellegehausen: Opt. Comm. 129 (1996), 134.
[2] S. Nolte, C. Momma, H. Jacobs, A. Tunnermann, B. N. Chichkov, B. Wellegehausen, H. Welling: J. Opt. Soc. Am. B, 14 (1997), 2716.
[3] H. K. Tönshoff, F. Von Alvensleben, A. Ostendorf, G. Kamlage, S. Nolte: IJEM Rev, 4 (1999), 1.
[4] X. Zhu, A. Naumov, D. Villeneuve, P. Corkum: Appl. Phys. A 69 (1999), 1.
[5] M. Weikert, C. Föhl, F. Dausinger, T. Abeln: Proc. SPIE 5063 (2003), 346.
[6] R. Le Harzic, N. Sanner, N. Huot, C. Donnet, E. Audouard, P. Laporte: Proc. SPIE 5063 (2003), 352.
[7] F. Dausinger: Proc. SPIE 4830 (2003), 471.
[8] R. Le Harzic, D. Breitling, M. Weikert, S. Sommer, C. Foehl, S. Valette, C. Donnet, E. Audouard, F. Dausinger: Appl. Surf. Sci. 249 (2005), 322.
[9] R. Le Harzic, D. Breitling, M. Weikert, S. Sommer, C. Foehl, F. Dausinger, S. Valette, C. Donnet, E. Audouard: Appl. Phys. A, 80 (2005),1589.
[10] R. Le Harzic, D. Breitling, S. Sommer, C. Föhl, K. König, F. Dausinger, and E. Audouard: Appl. Phys. A 81 (2005) 1121.
[11] W. Denk, J.H. Strickler, W.W.Webb: Science 248 (1990), 73.
[12] K. König: J. Microsc. 200 (2000), 83.
[13] K. König, I. Riemann: JBO 8 (2003) 432.
[14] K. König, I. Riemann, W. Fritzsche: Opt. Lett. **26** (2001), 819.
[15] B. Tirlapur, K. König: Nature 418 (2002), 290.
[16] K. König, O. Krauss, I. Riemann: Optics Express 10 (2002), 171.
[17] K. König, I. Riemann, F. Stracke, R. LeHarzic: Lasers in Medical Applications 20 (2005) 169.
[18] K. König, F. Bauerfeld, D. Sauer, H. Schuck, A. Uchugonova, E. Lai, M. Stark, T. Velten, R. Bückle, R. Le Harzic, Handai Nanophotonics vol. 3, ed. by H. Masuhara, S. Kawata and F. Tokunaga(Publisher, Elsevier, 2007) p.287. (Books)

[19] R. Le Harzic, D. Sauer, I. Riemann, K. König: Proc. SPIE 5989, (2005), 189.
[20] J. Pedraza, J. D. Fowlkes and D. H. Lowndes: Appl. Phys. A 69 (1999), 731.
[21] J. Pedraza, J. D. Fowlkes and Y. F. Guan: Appl. Phys. A 77 (2003), 277.
[22] W.Kautek, P. Rudolph, G. Daminelli and J. Krüger: Appl. Phys. A. 81 (2005), 65.
[23] R. Le Harzic, H. Schuck, D. Sauer, T. Anhut, I. Riemann, T. Velten, K. König: Optics Express, 13 (2005), 6651.
[24] R. An, Y. Li, Y. Dou, H. Yang, Q. Gong: Optics Express 13 (2005), 1855.
[25] Y. Bellouard, A. Said, M. Dugan, P. Bado: Optics Express 12 (2004), 2120.
[26] Y. Cheng, K. Sugioka, K. Midorikawa: Opt. Lett 29 (2004), 2007.
[27] K. Ke, E. F. Hasselbrink, A. J. Hunt: Anal. Chem 77 (2005), 5083.
[28] P. Becker, D. Sauer, F. Bauerfeld, K. König, R. Le Harzic: Proc. SPIE 6879 (2008).
[29] K. König, H. Schuck, D. Sauer, F. Bauerfeld, F. Stracke, T. Velten, A. Tchernook, S. Martin, R. Le Harzic: Proc. SPIE 6400 (2006).
[30] E. Lai, Master thesis (2007).
[31] R.G. Flemming, C.J. Murphy, G.A. Abrams, S.L. Goodman, P.F. Nealey: Biomaterials 20 (1999).
[32] A. Curtis and C. Wilkinson: Biomaterials 18 (1997).

(Received: April 24, 2007, Accepted: March 17, 2008)